Supplement of Atmos. Chem. Phys., 20, 2839–2863, 2020
https://doi.org/10.5194/acp-20-2839-2020-supplement

Atmospheric Chemistry and Physics
Open Access

Supplement of

Modeling diurnal variation of surface $PM_{2.5}$ concentrations over East China with WRF-Chem: impacts from boundary-layer mixing and anthropogenic emission

Qiuyan Du et al.

Correspondence to: Chun Zhao (chunzhao@ustc.edu.cn)

Supporting materials for "Modeling diurnal variation of surface $PM_{2.5}$ concentration over East China with WRF-Chem: Impacts from boundary layer mixing and anthropogenic emission"

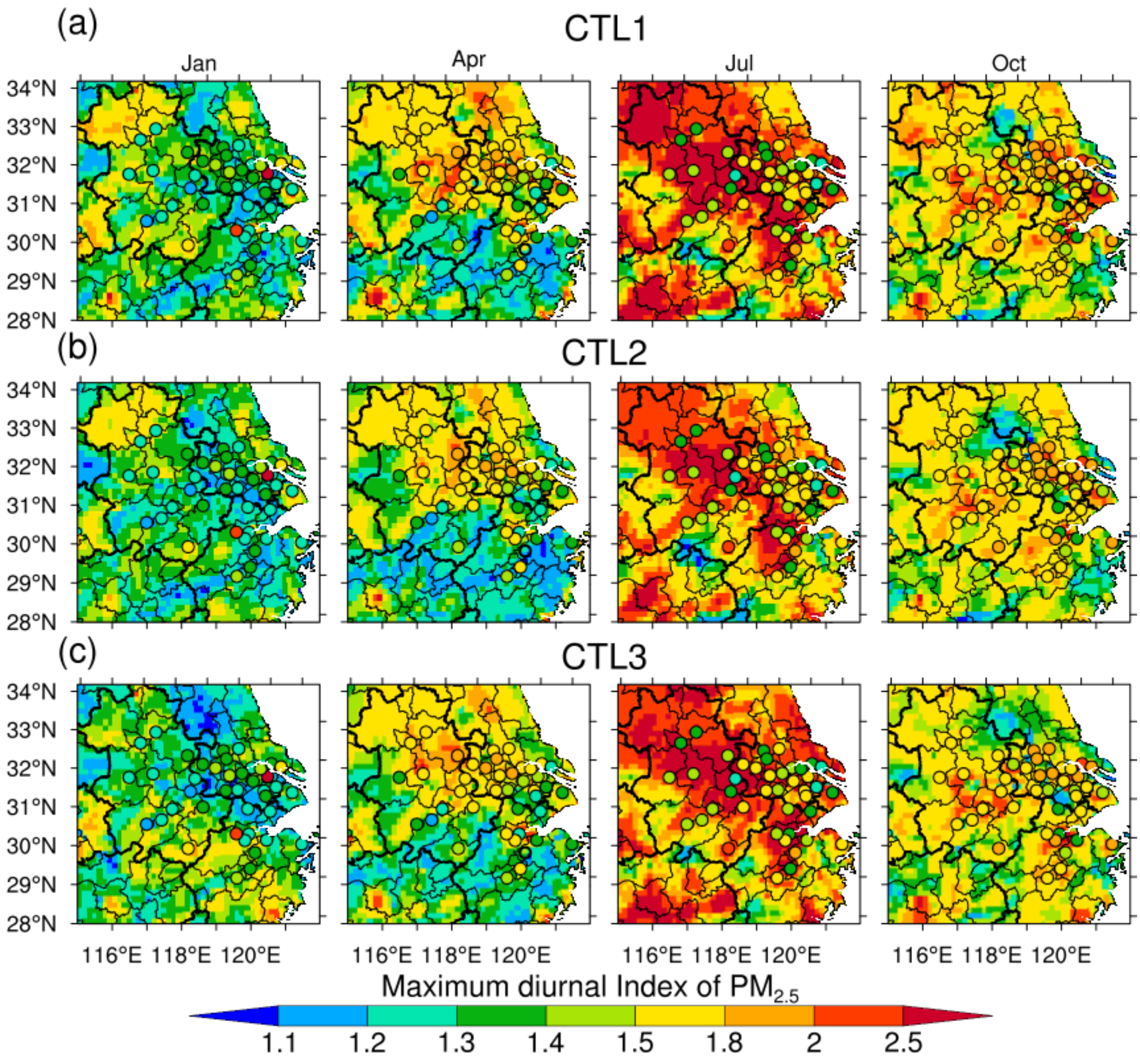

Figure S1. Spatial distribution of peak diurnal index of surface $PM_{2.5}$ concentrations in the four months from experiments CTL1, CTL2, and CTL3. The observations are shown as the color filled circles. The observations at the stations within one city are averaged and shown as one circle as they are too close to be shown distinctly.

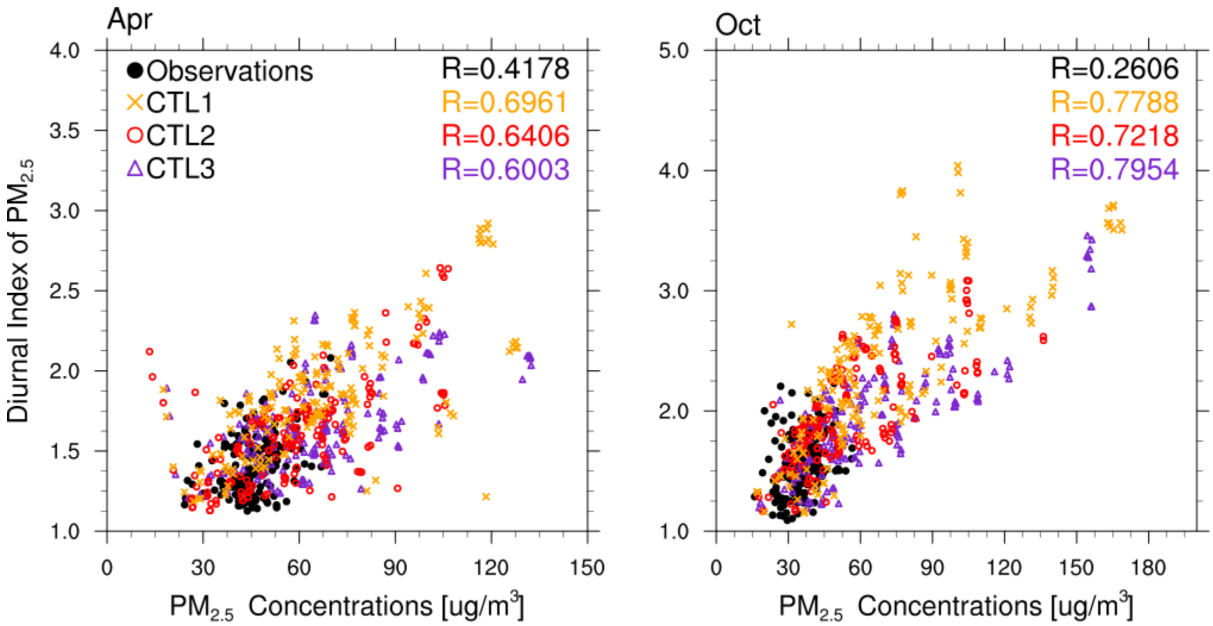

Figure S2. Comparison between monthly mean surface $PM_{2.5}$ concentrations and diurnal index of surface $PM_{2.5}$ concentrations at each observational site over the YRD region of East China (within black box of Fig. 1a) for April and October from observations and experiments CTL1, CTL2, and CTL3.

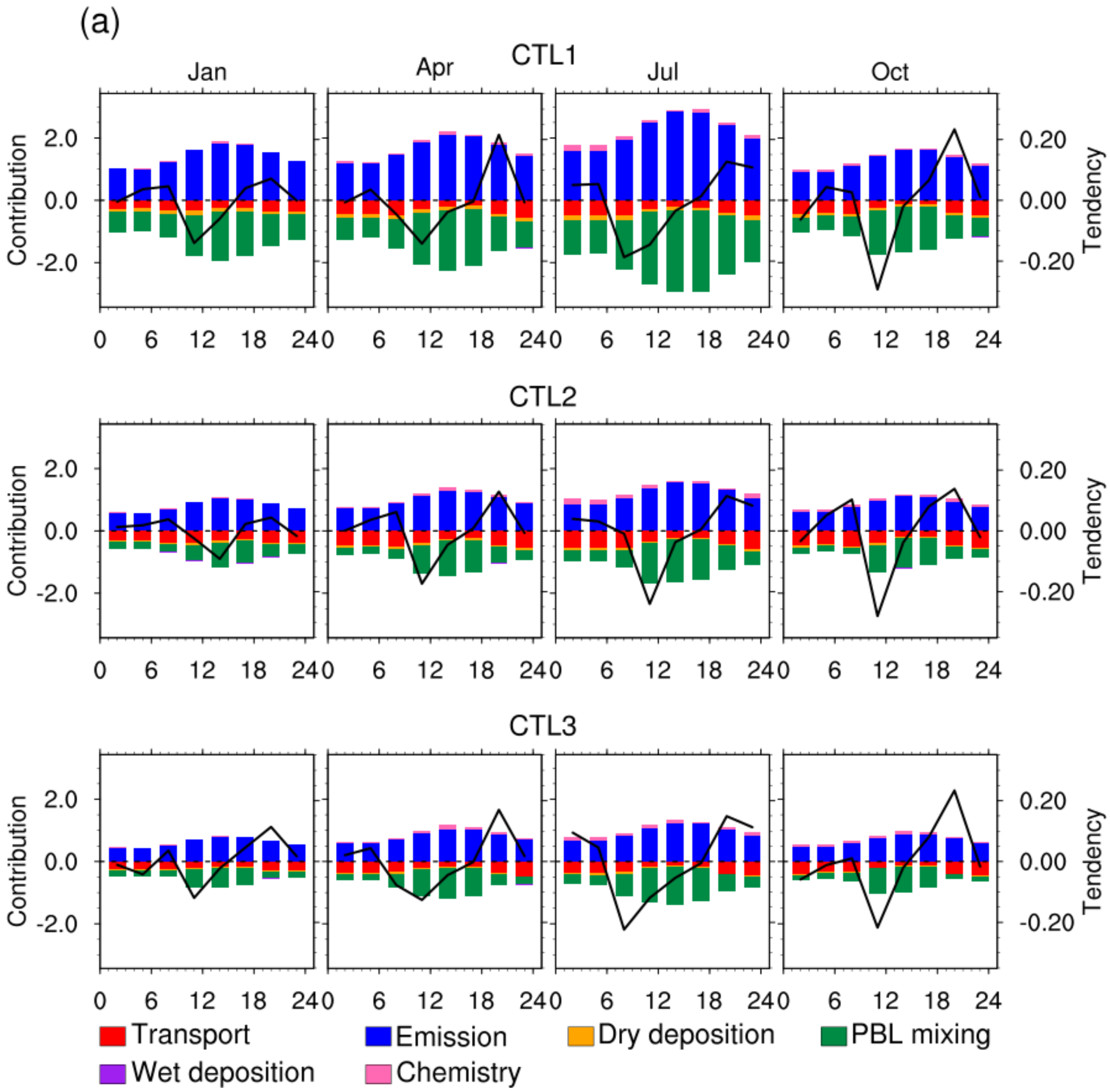

Figure S3a. Relative contribution (normalized by monthly mean surface $PM_{2.5}$ concentrations for each month) to surface $PM_{2.5}$ concentrations every 3-hour from individual process (transport, emission, dry and wet deposition, PBL mixing, chemical production/loss) averaged over Nanjing(a) for January, April, July, and October of 2018 from experiments CTL1, CTL2, and CTL3. The 3-hourly relative tendency of surface $PM_{2.5}$ concentrations is also shown as the black line.

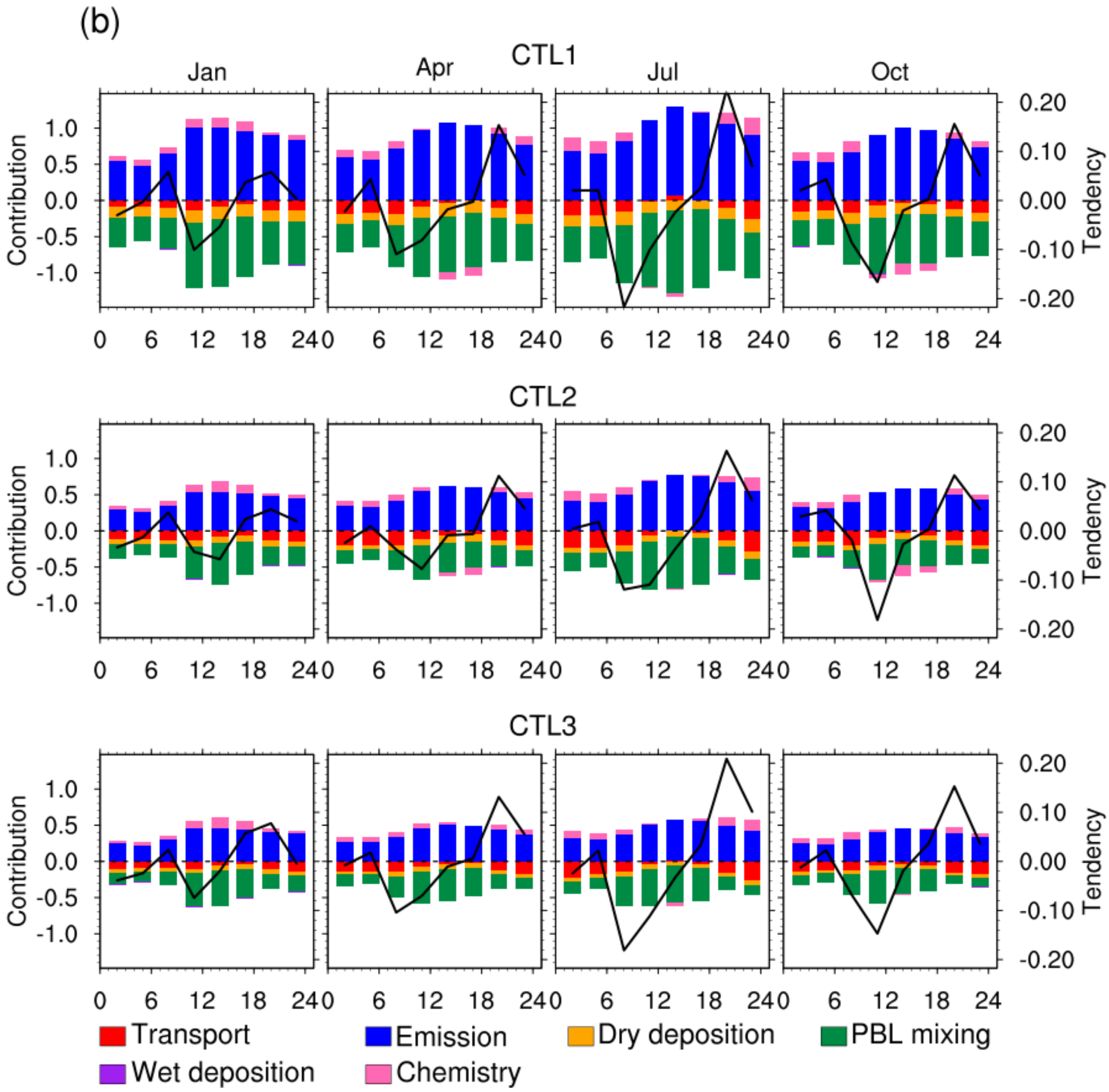

Figure S3b. Same as Fig. S3a but for Hangzhou.

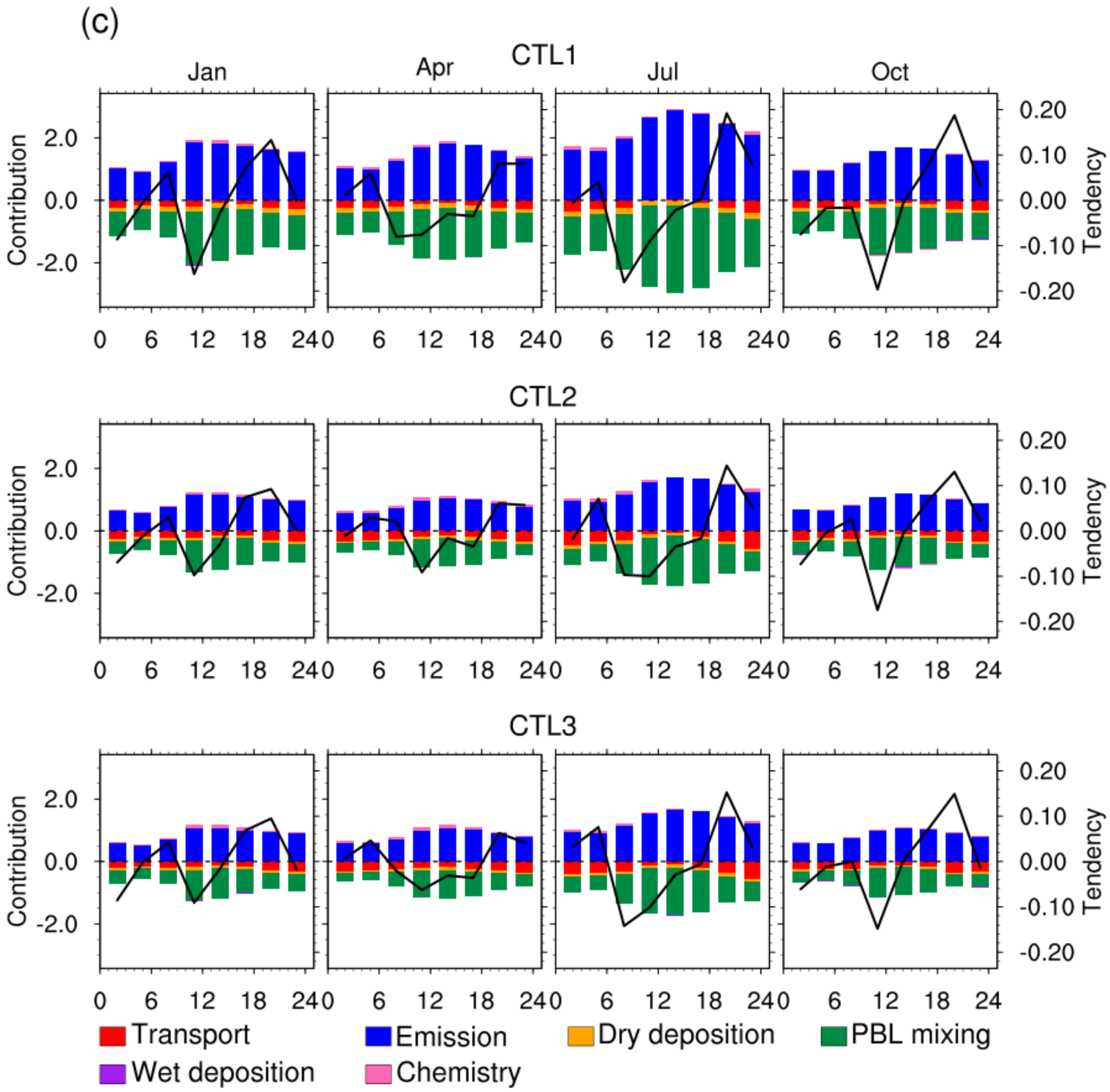

Figure S3c. Same as Fig. S3a but for Shanghai.

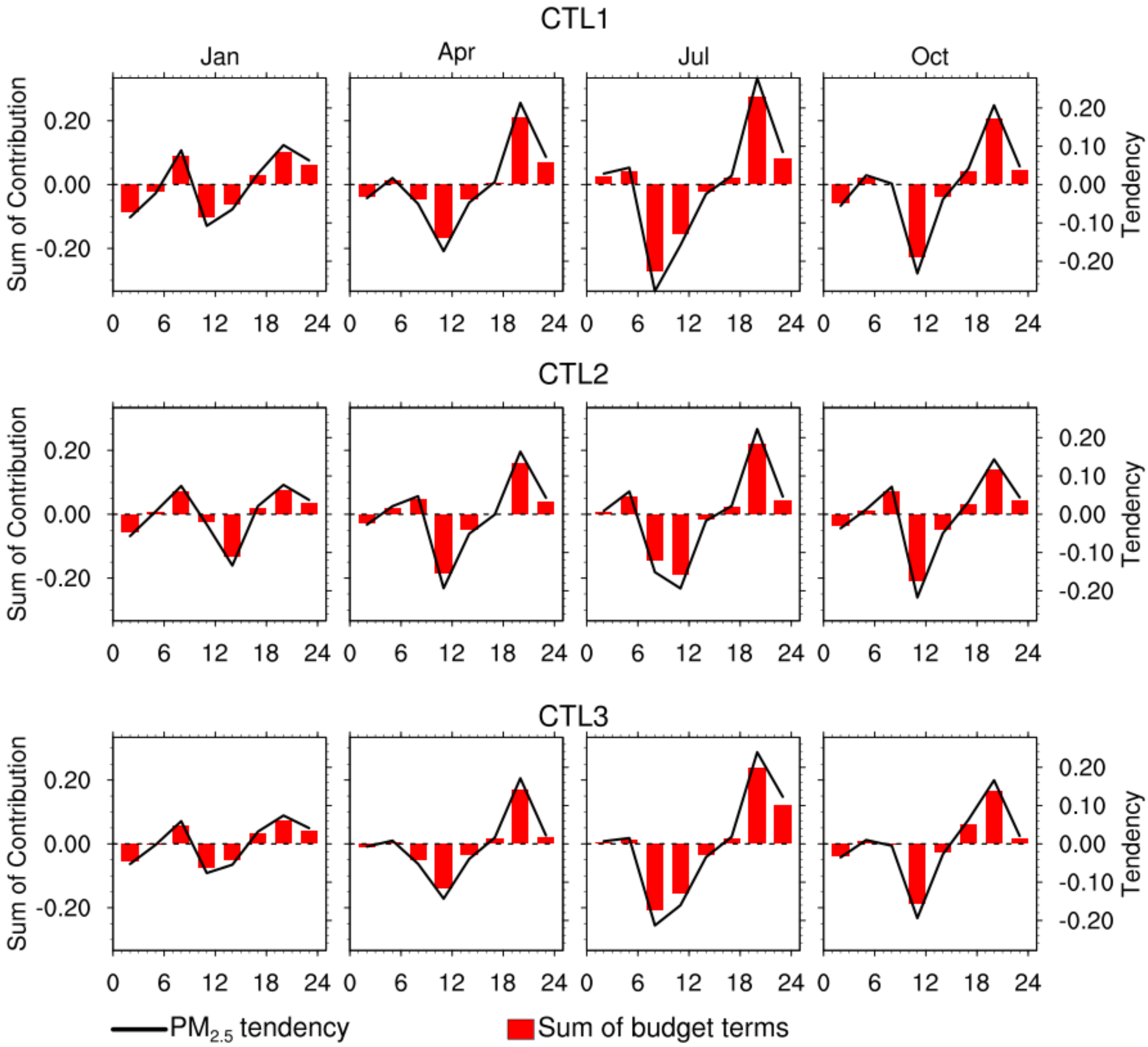

Figure S4. Validation of the consistency between summation of relative contributions from processes and the relative tendency of surface $PM_{2.5}$ concentration averaged over Hefei for January, April, July, and October of 2018 from experiments CTL1, CTL2, and CTL3.

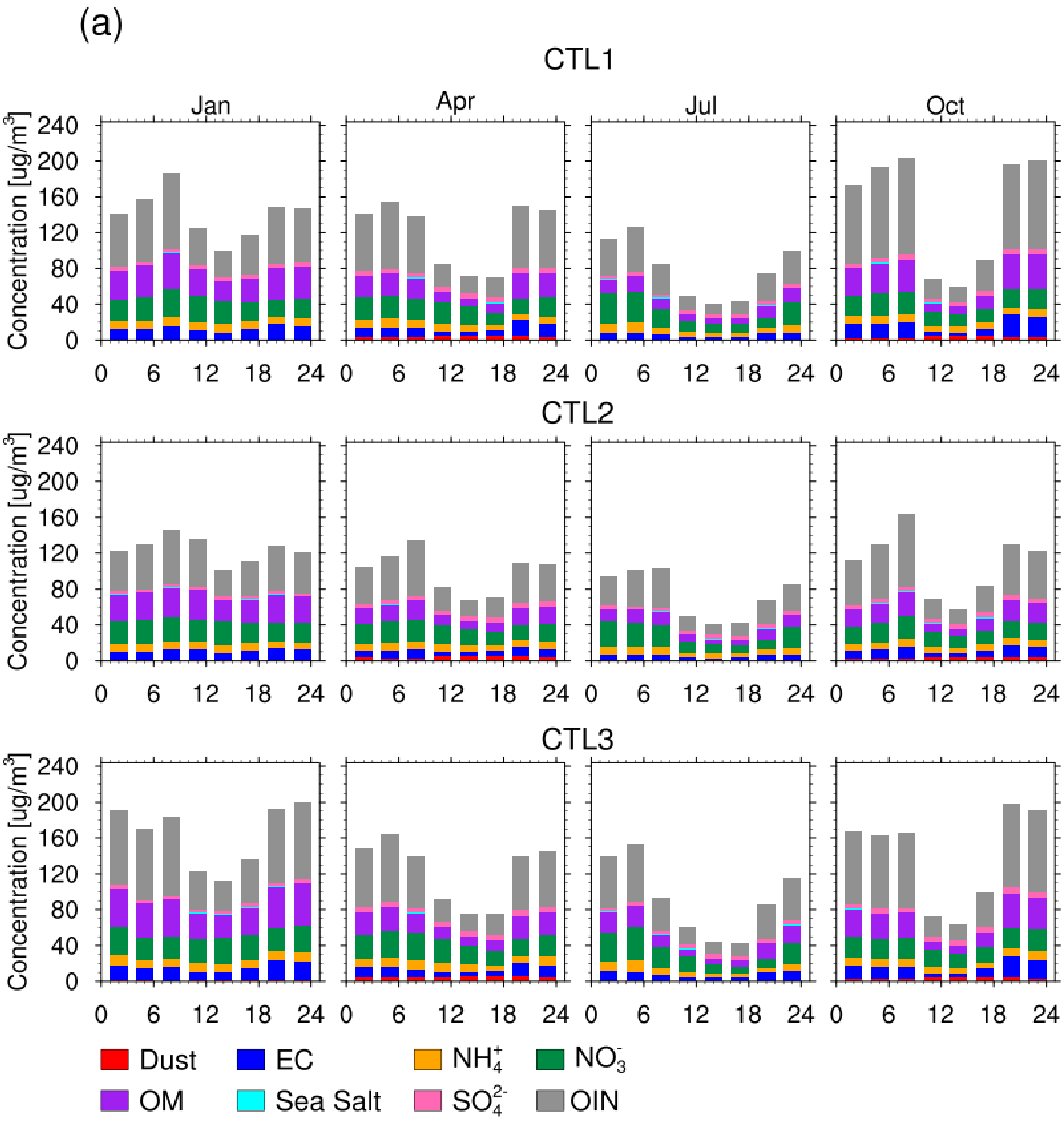

Figure S5a. Diurnal variation of surface concentration of each $PM_{2.5}$ composition (Dust, OM, EC, Sea Salt, NH_4^+, SO_4^{2-}, NO_3^-, and other inorganics) averaged over Nanjing(a) for January, April, July, and October of 2018 from experiments CTL1, CTL2, and CTL3.

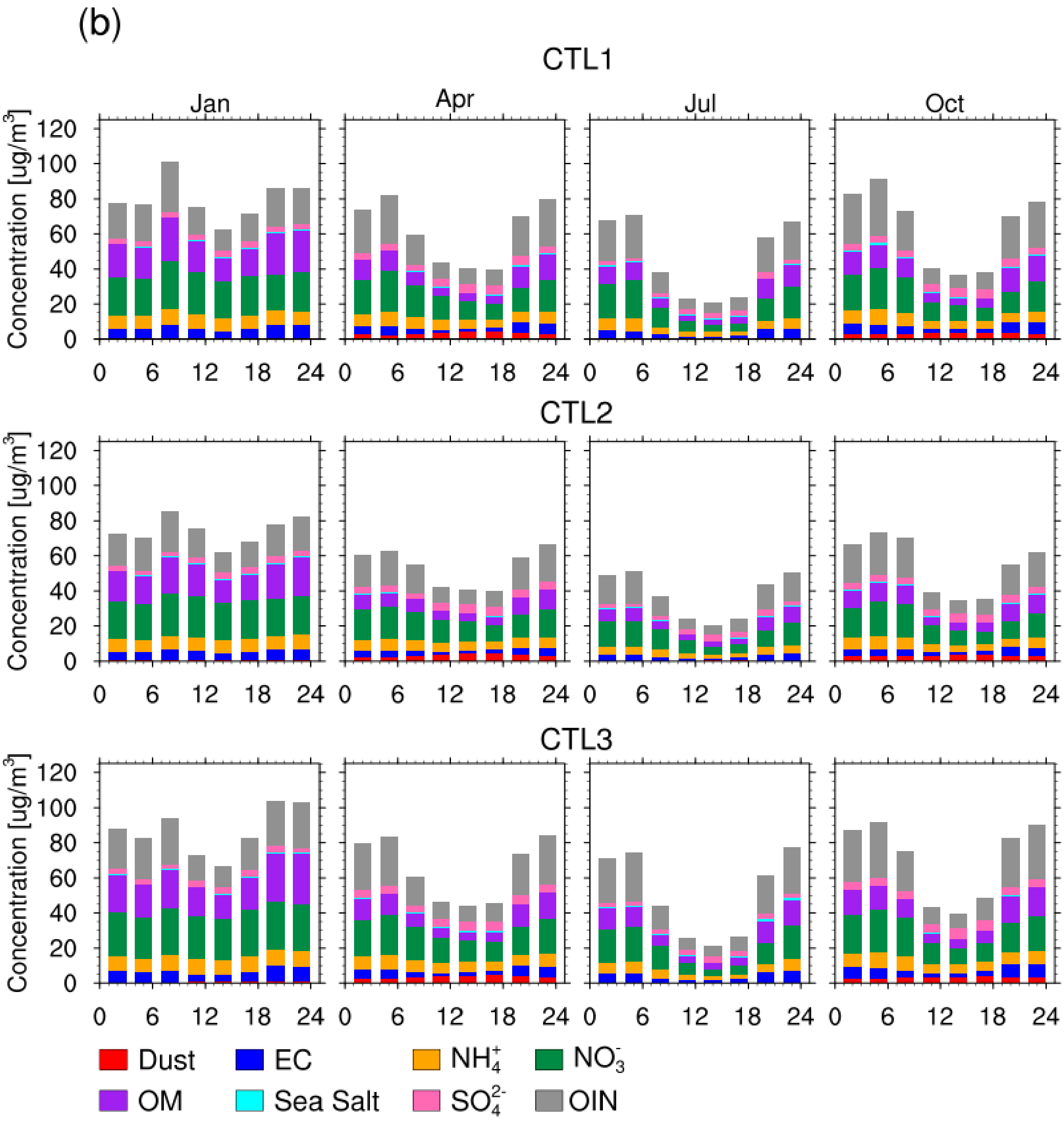

Figure S5b. Same as Fig. S5a but for Hangzhou.

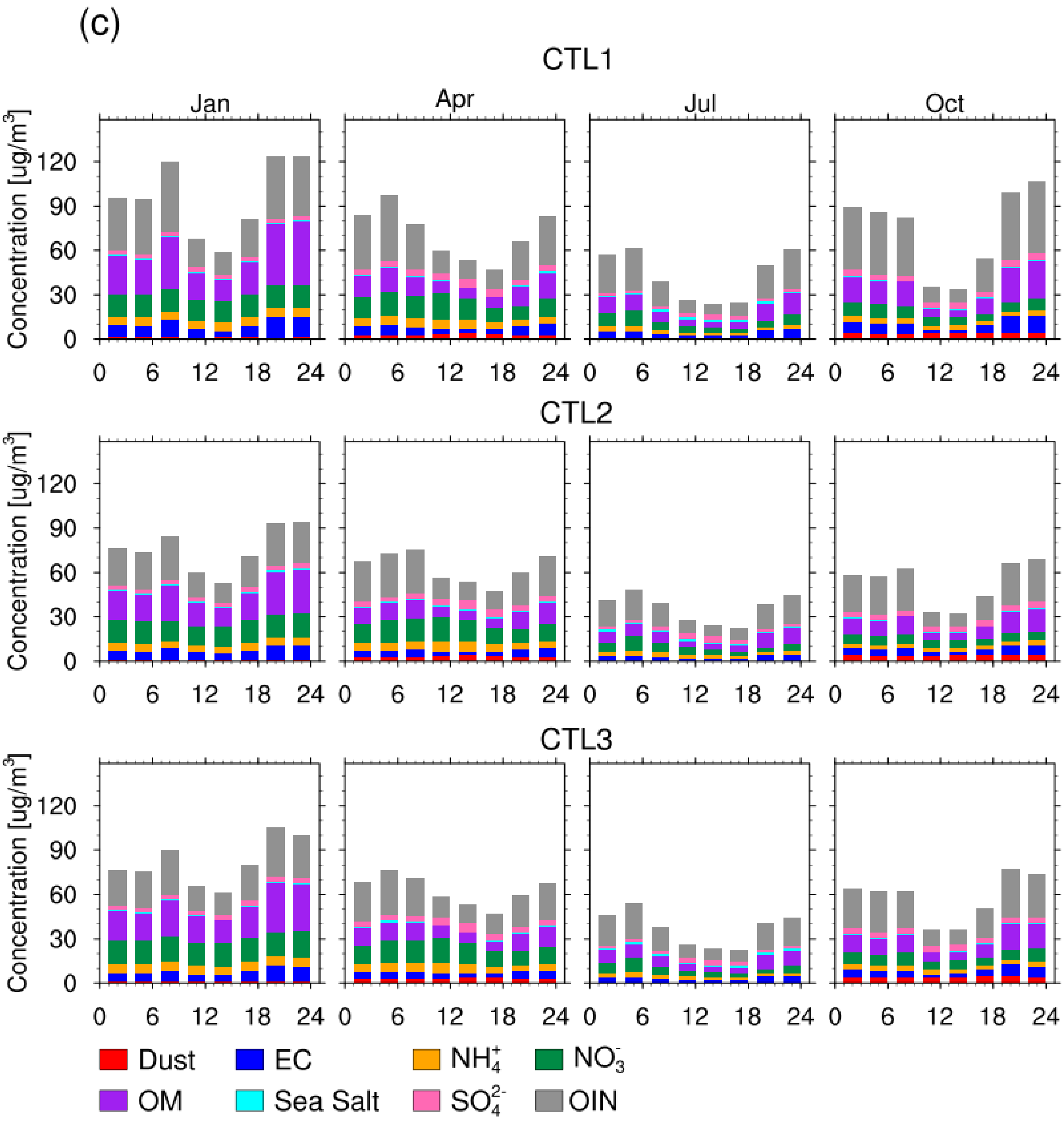

Figure S5c. Same as Fig. S5a but for Shanghai.

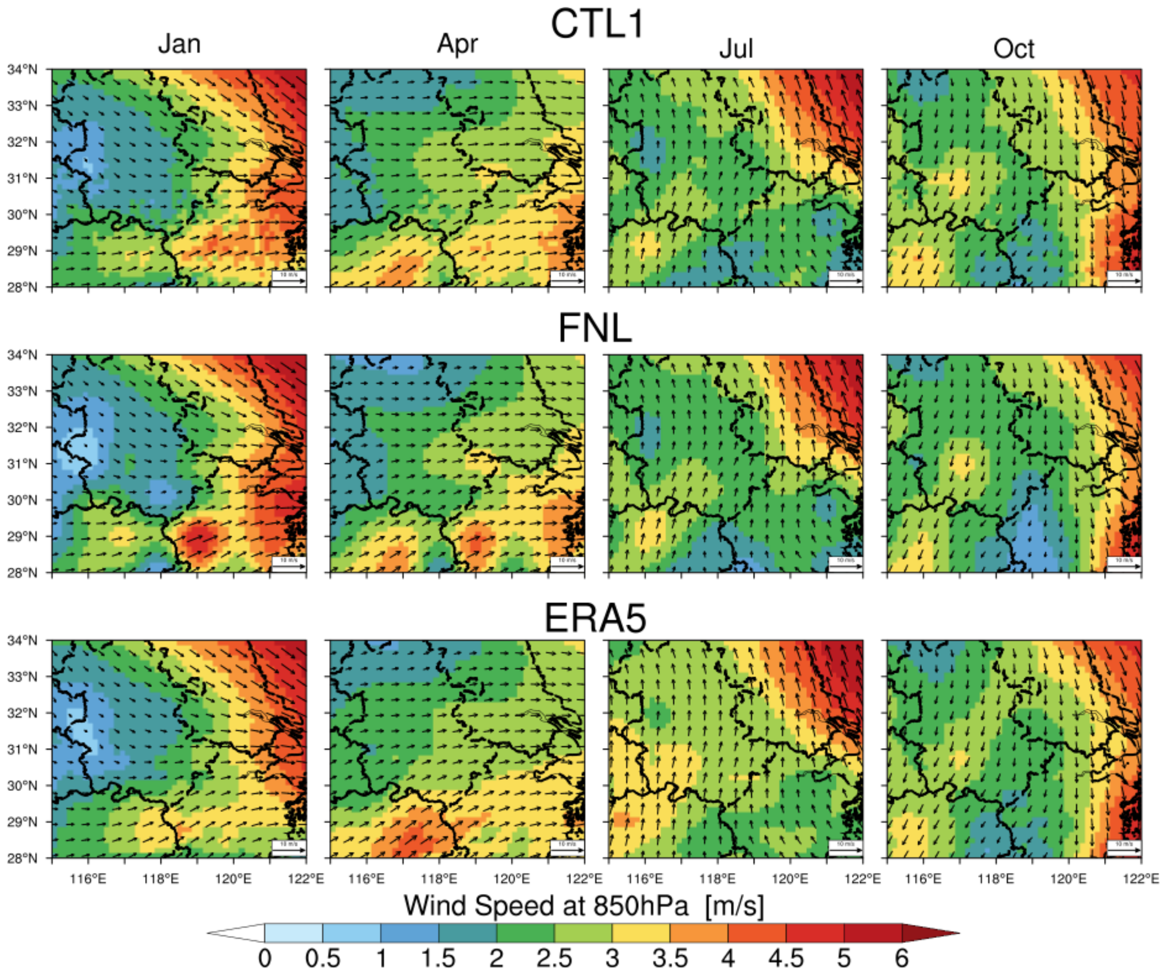

Figure S6. Spatial distribution of wind speeds at 850 hPa from the experiment CTL1 and FNL and ERA5 reanalysis datasets over East China averaged for January, April, July, and October of 2018.

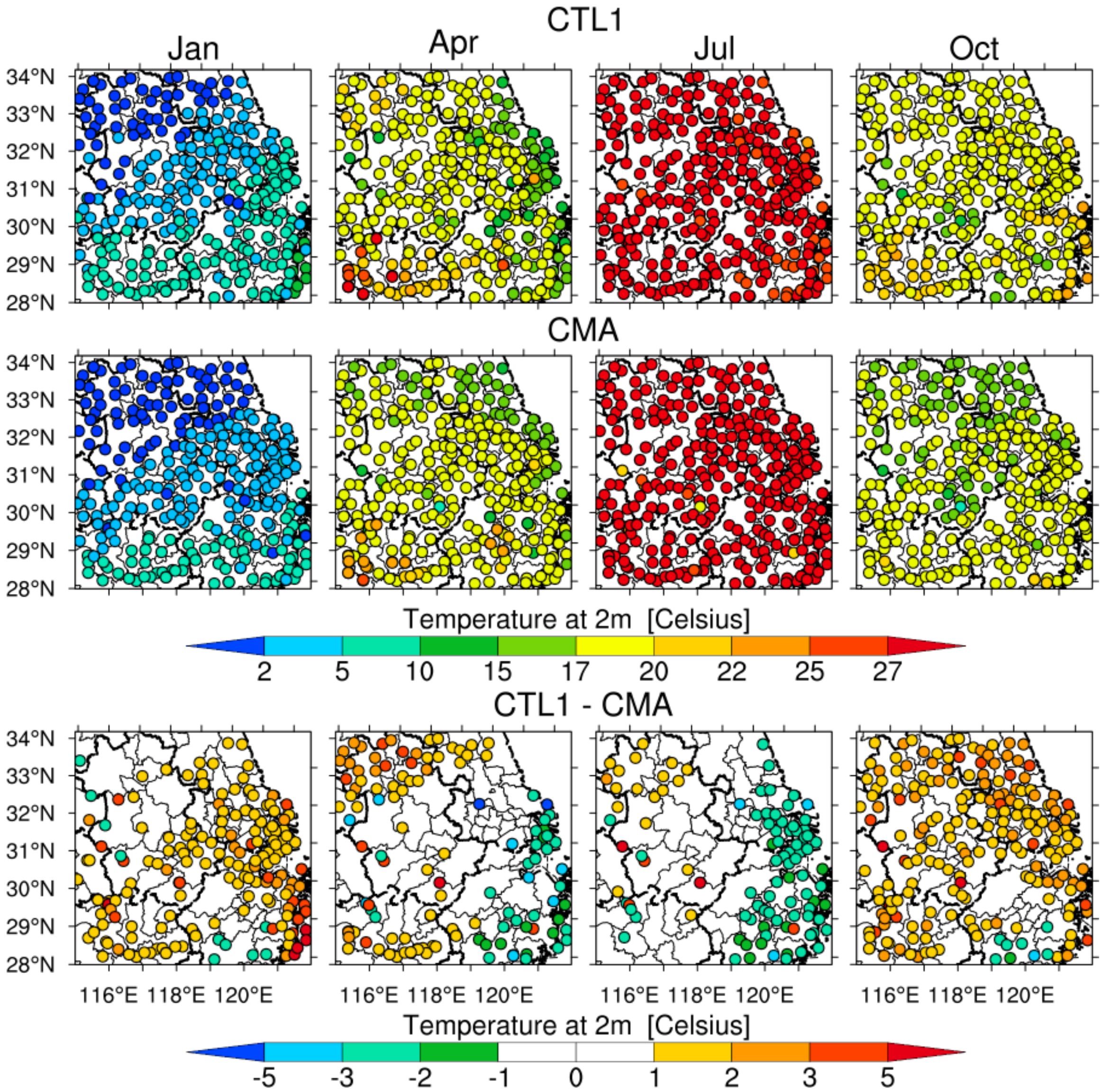

Figure S7. Spatial distribution of temperature at 2m from the experiments CTL1 and the CMA observations at the stations of East China for January, April, July, and October of 2018.

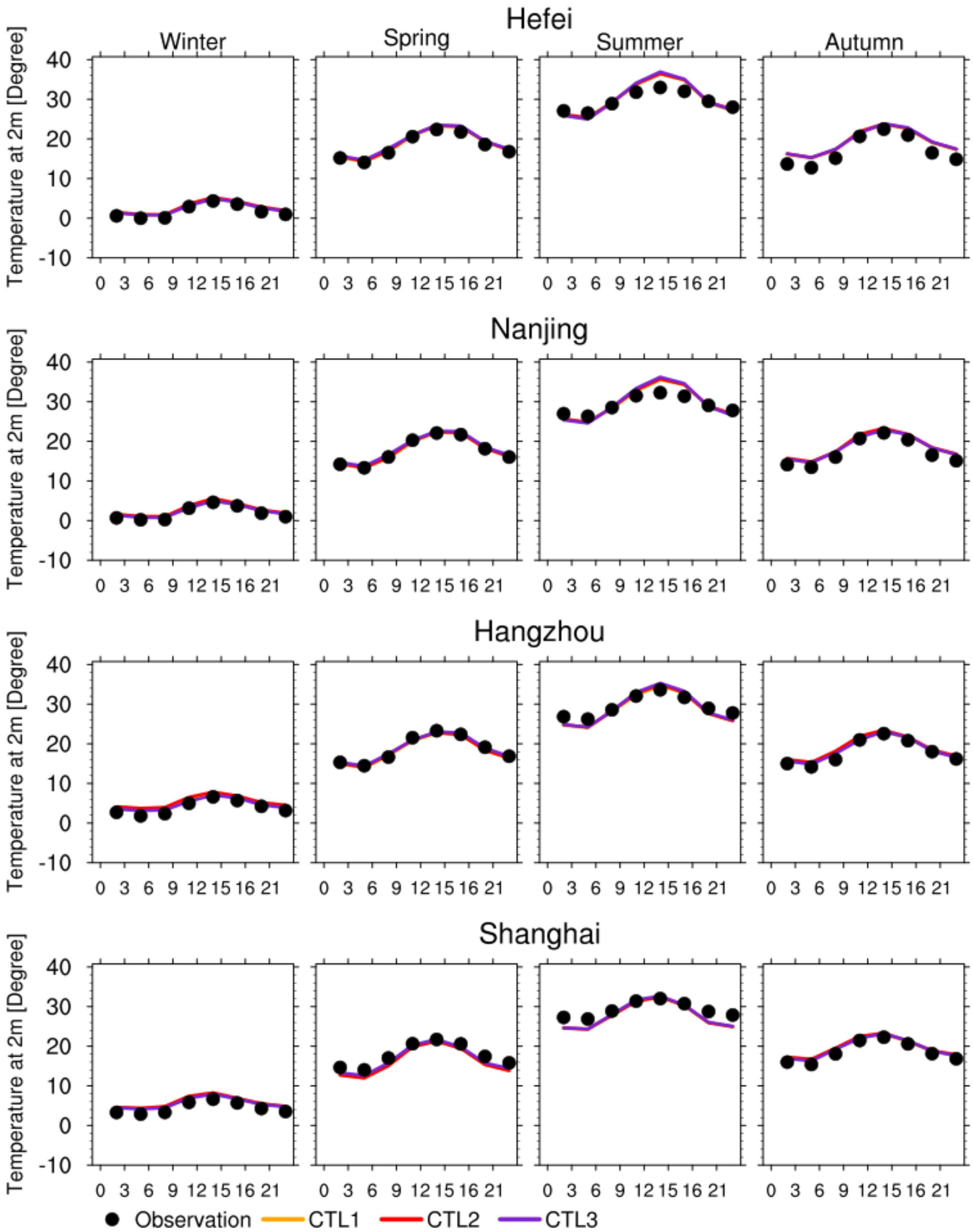

Figure S8. Diurnal variation of temperature at 2m within 24-hour averaged over four cities (Hefei, Nanjing, Hangzhou, Shanghai) for January, April, July, and October of 2018 from experiments CTL1, CTL2, and CTL3, and CMA observations.

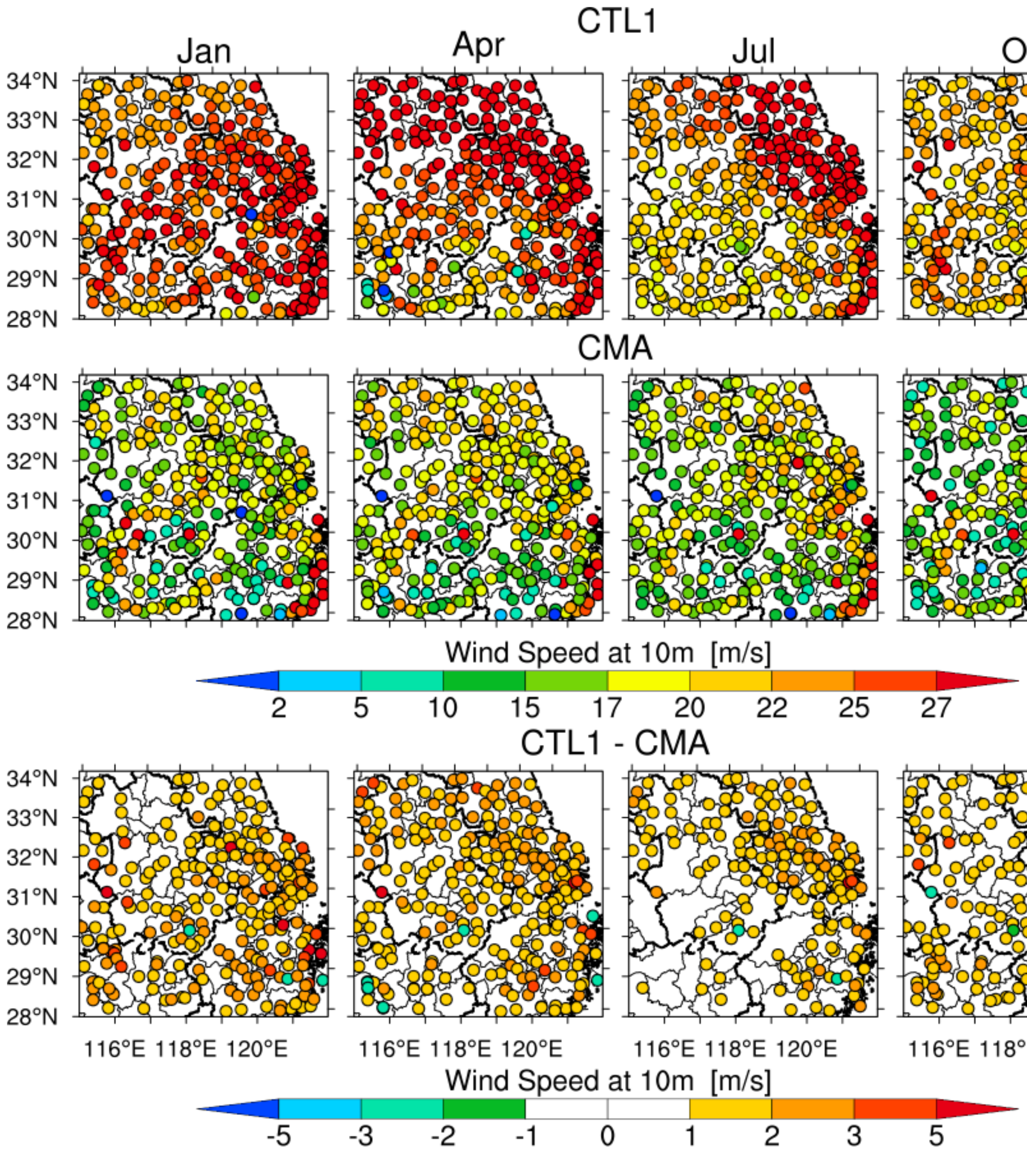

Figure S9. Spatial distribution of wind speeds at 10m from the experiment CTL1 and the CMA observations at the stations of East China for January, April, July, and October of 2018.

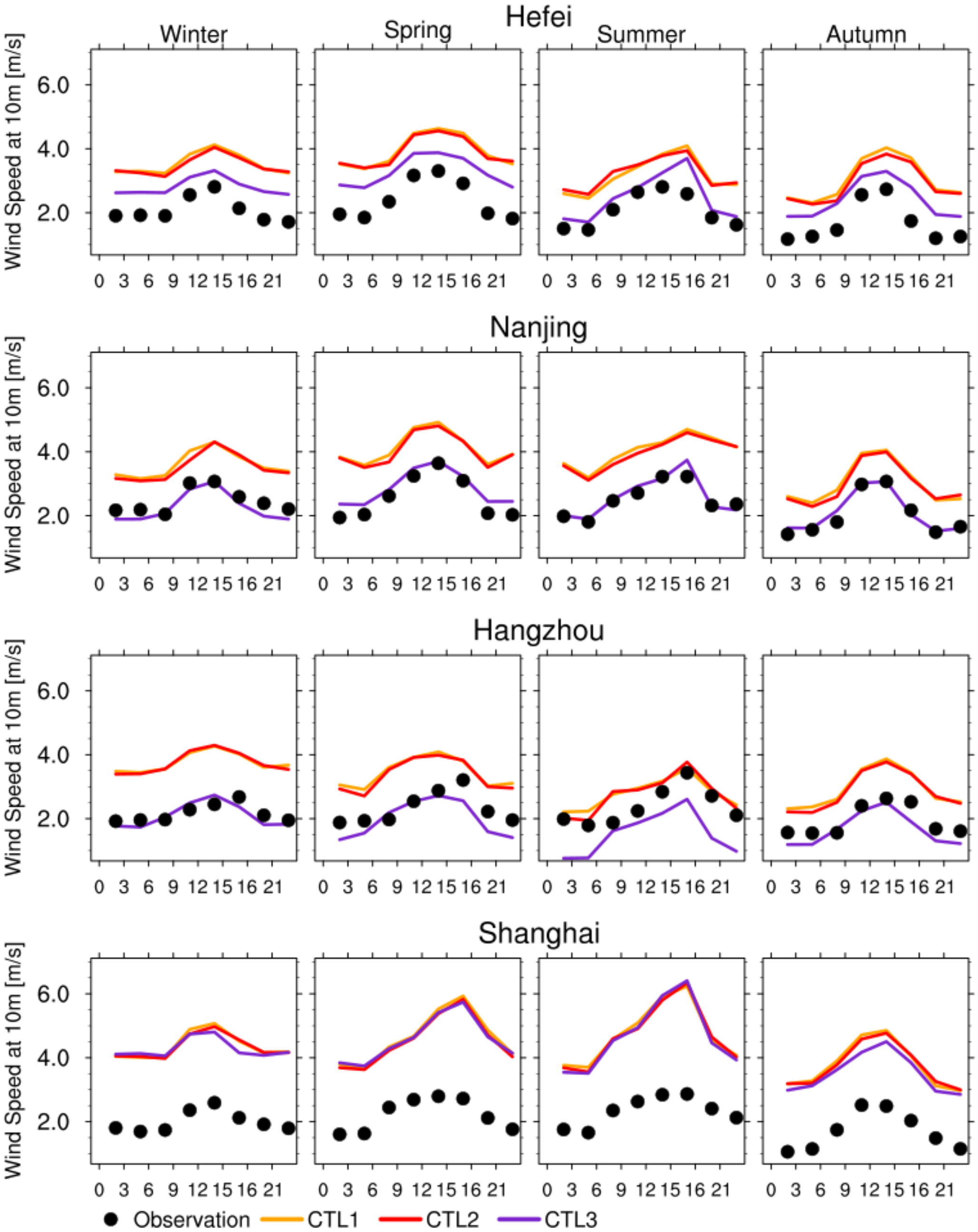

Figure S10. Diurnal variation of wind speeds at 10m within 24-hour averaged over four cities (Hefei, Nanjing, Hangzhou, and Shanghai) for January, April, July, and October of 2018 from experiments CTL1, CTL2, and CTL3 and CMA observations.

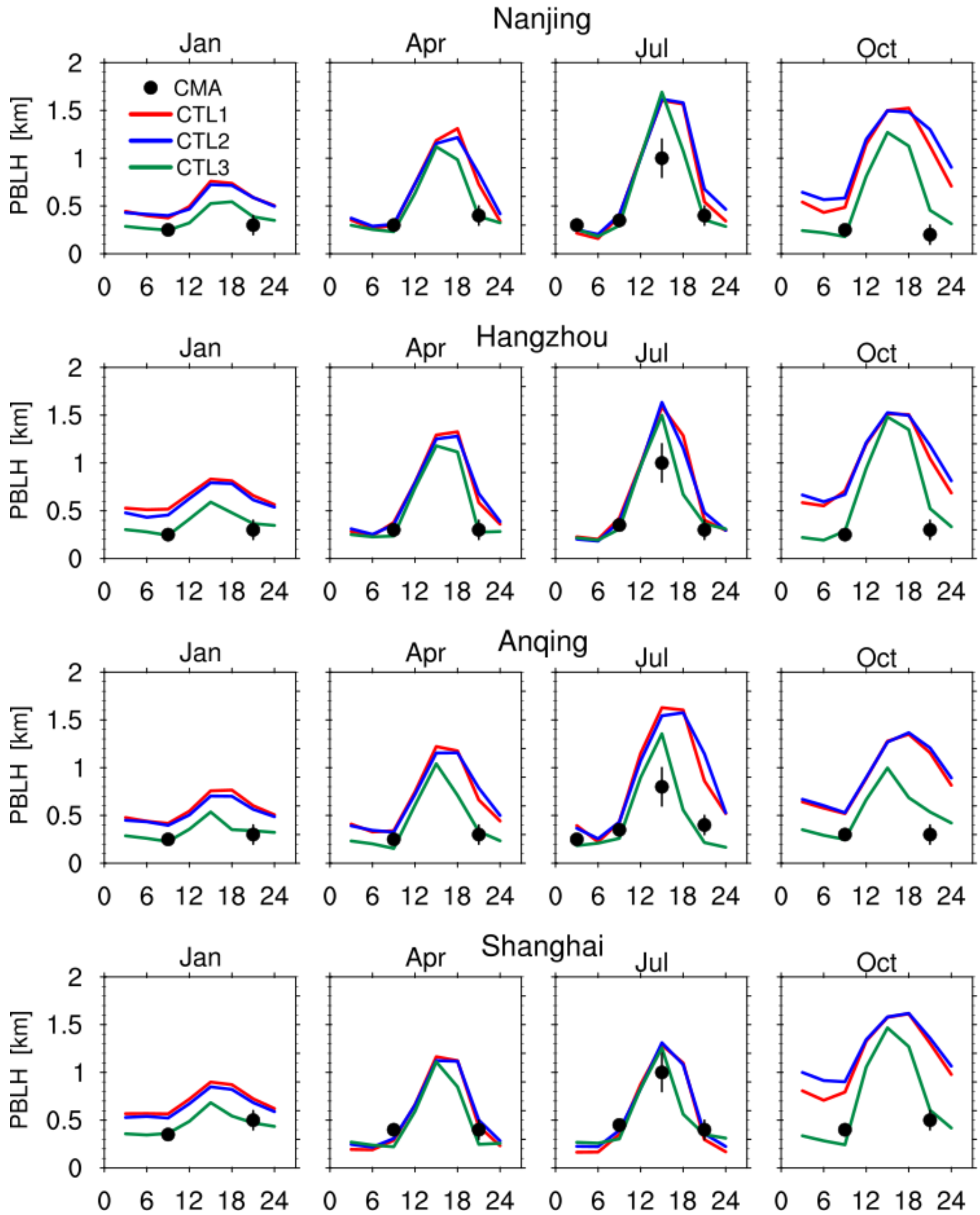

Figure S11. Diurnal variation of PBL height within 24-hour averaged at four stations in the cities of Nanjing, Hangzhou, Anqing, and Shanghai, respectively, for January, April, July, and October of 2018 from experiments CTL1, CTL2, and CTL3. The long-term PBL heights at specific time derived from the air sounding observations at the corresponding stations are also shown as the black solid circle.

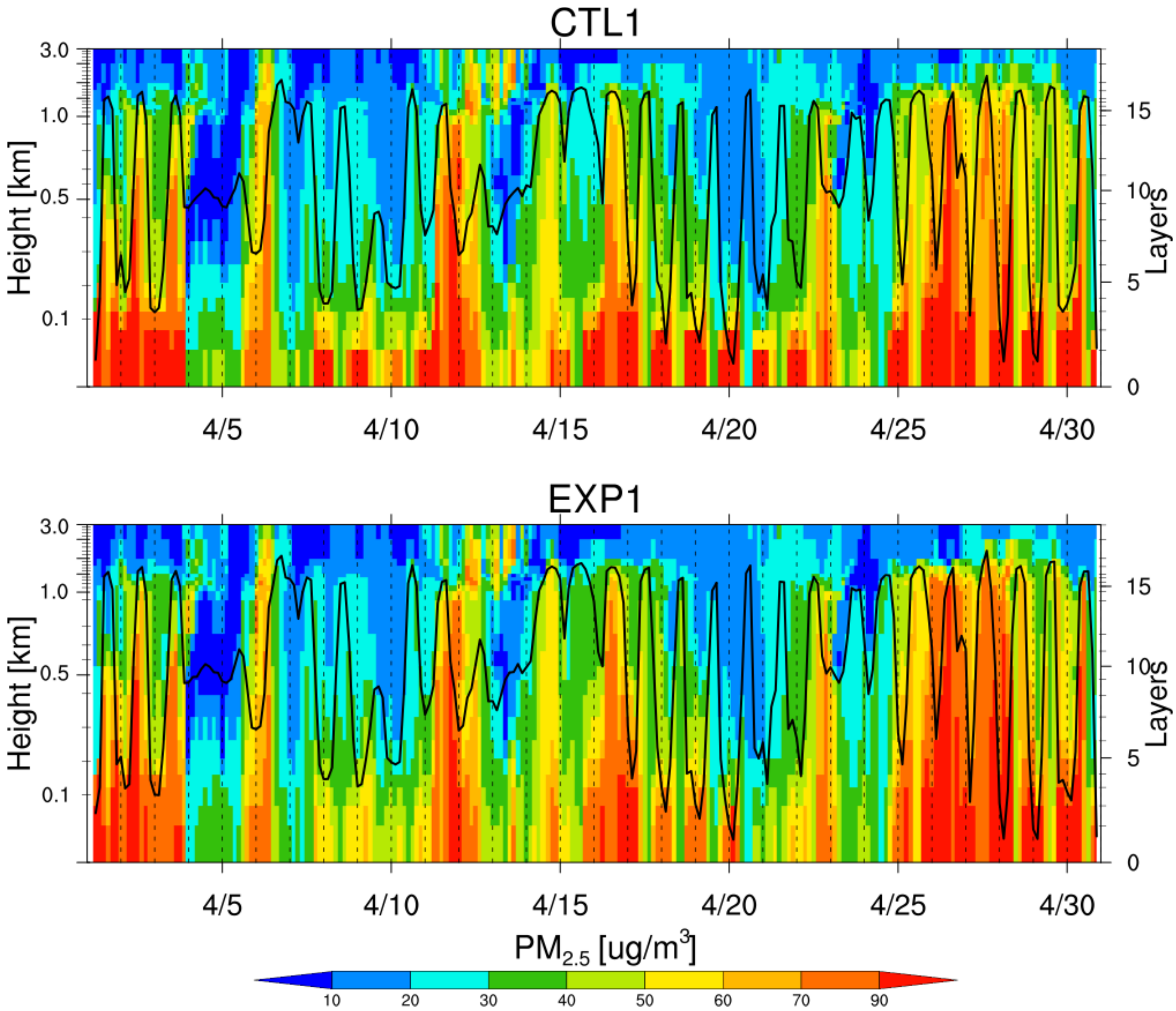

Figure S12. 3-hourly variation of PBLH and vertical distributions of $PM_{2.5}$ concentrations at Hefei in April of 2018 from the experiment CTL1 and EXP1.

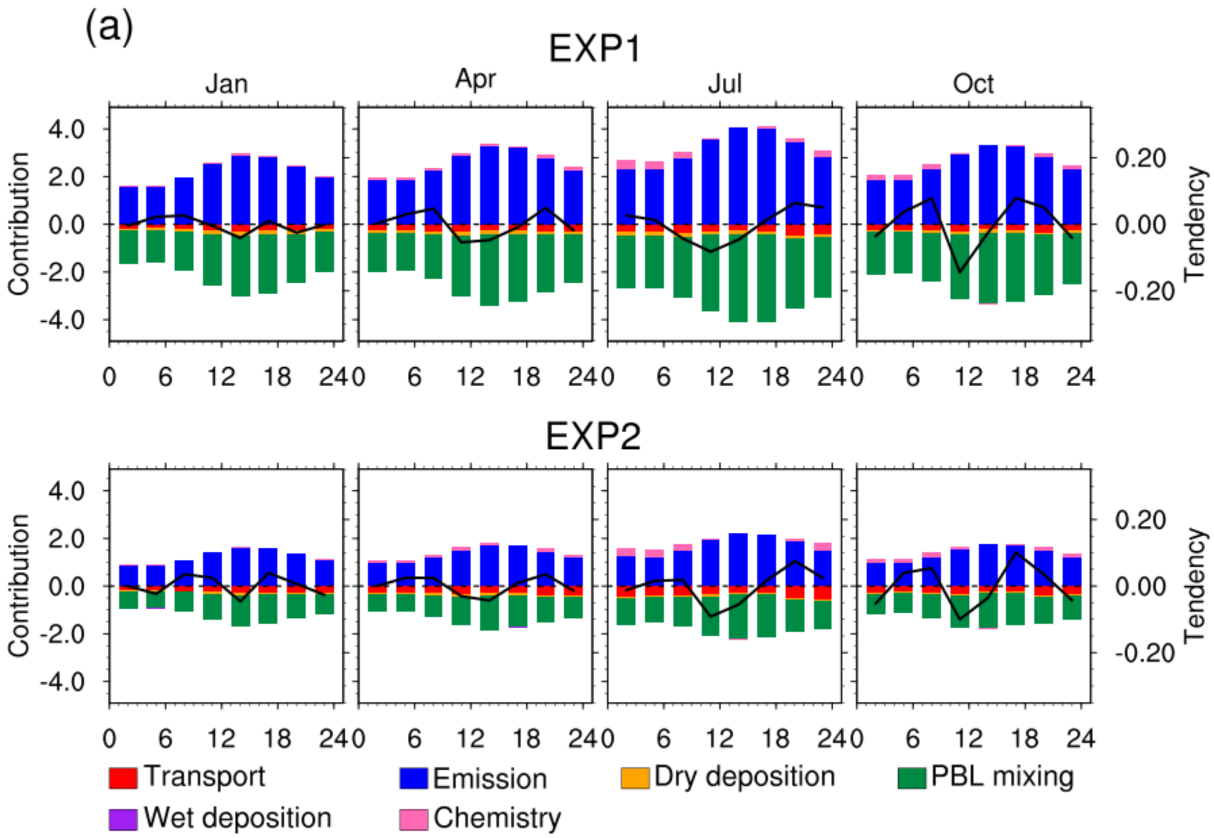

Figure S13a. Relative contribution (normalized by monthly mean surface PM2.5 concentrations for each month) to surface PM2.5 concentrations every 3-hour from individual process (transport, emission, dry and wet deposition, PBL mixing, chemical production/loss) averaged over Nanjing(a) for January, April, July, and October of 2018 from experiments EXP1 and EXP2. The 3-hourly relative tendency of surface PM2.5 concentrations is also shown as the black line.

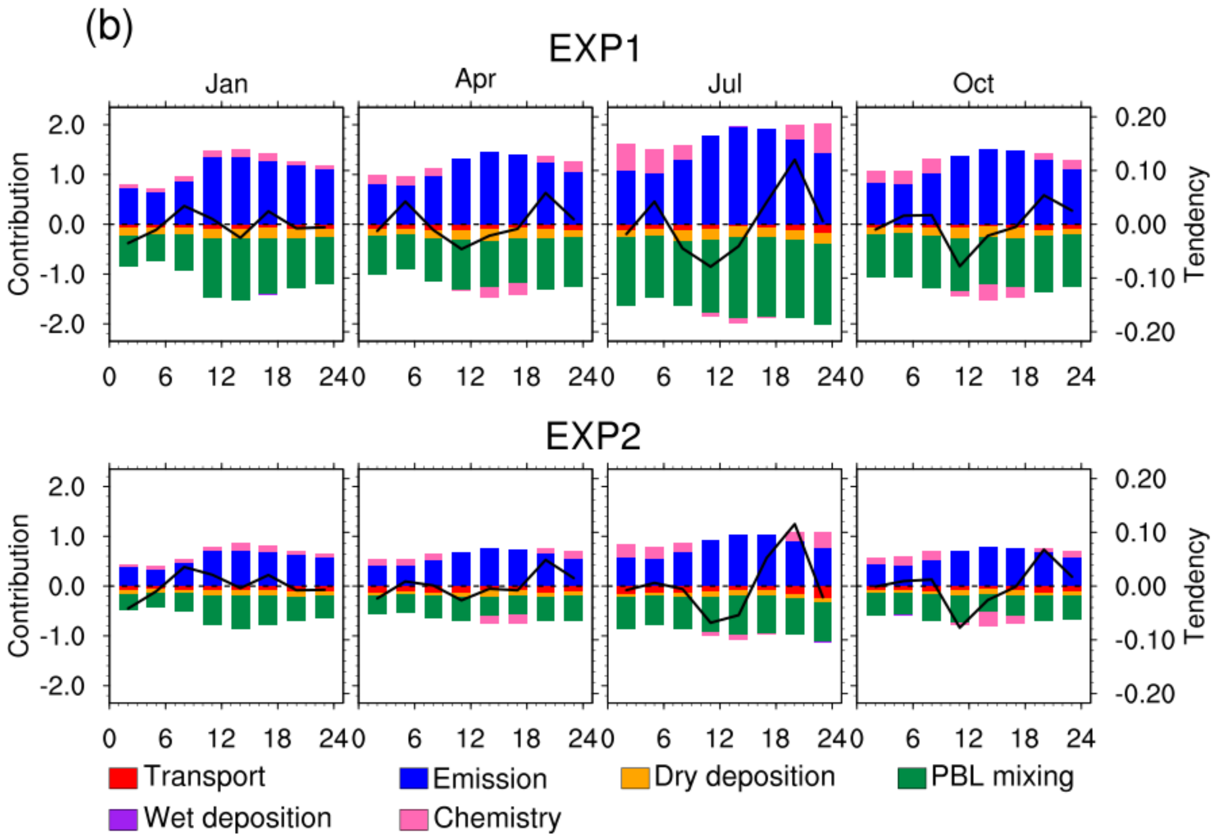

Figure S13b. Same as Fig. S13a but for Hangzhou.

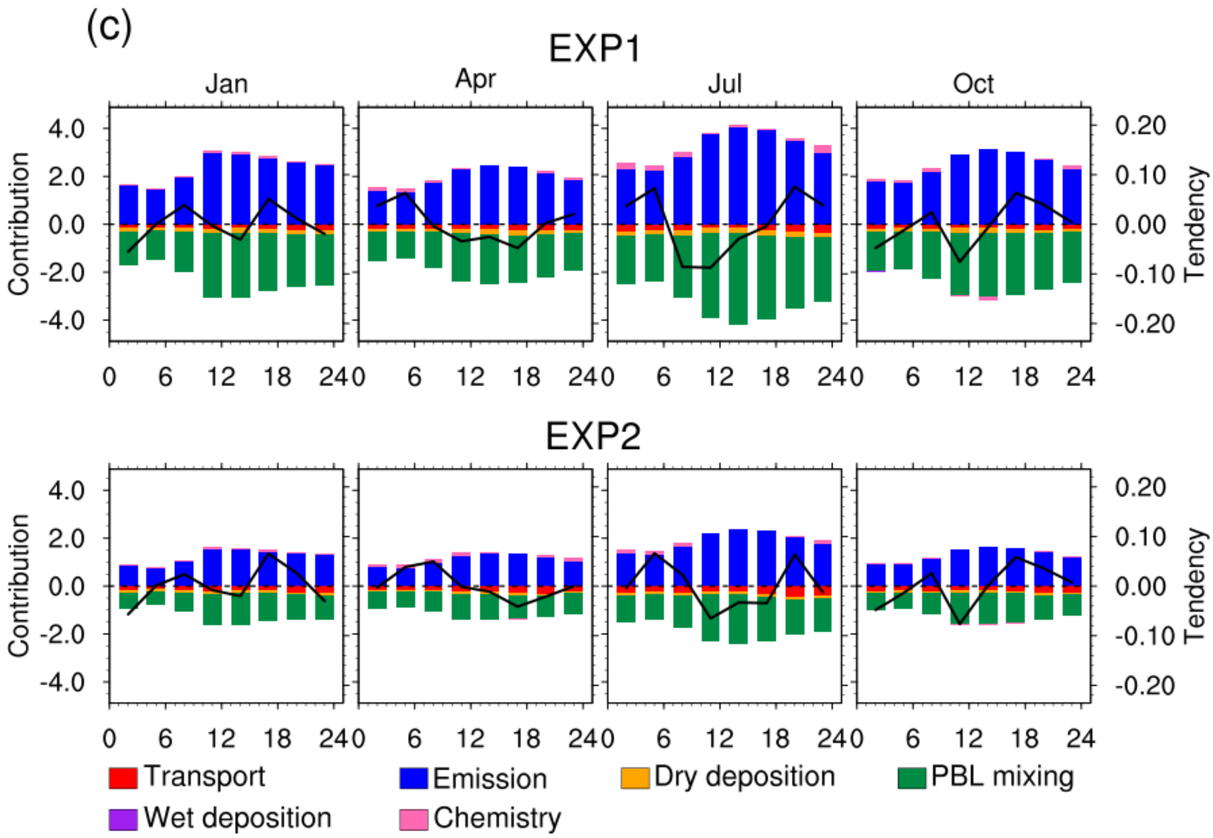

Figure S13c. Same as Fig. S13a but for Shanghai.

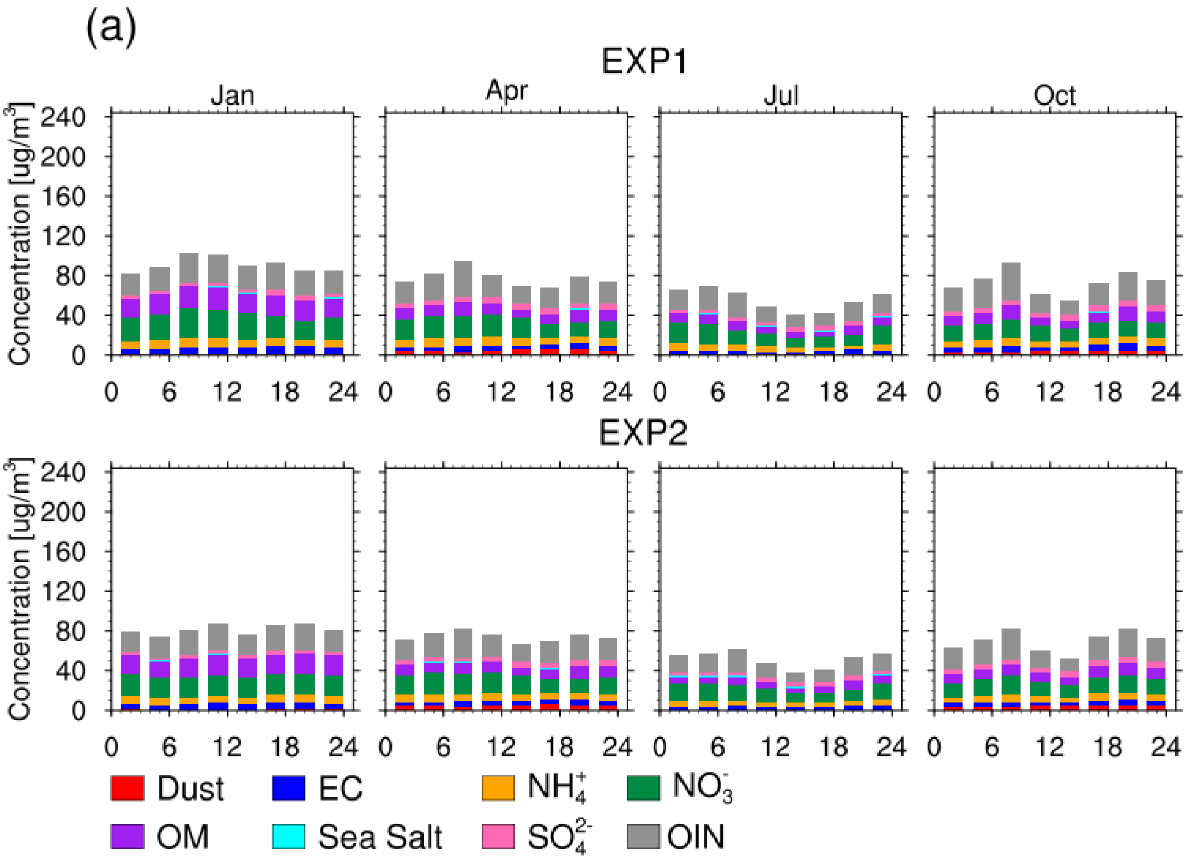

Figure S14a. Diurnal cycle of surface PM2.5 composition concentrations (Dust, OM, EC, Sea Salt, NH_4^+, SO_4^{2-}, NO_3^-, and other inorganics) averaged over Nanjing(a) for January, April, July, and October of 2018 from experiments EXP1 and EXP2.

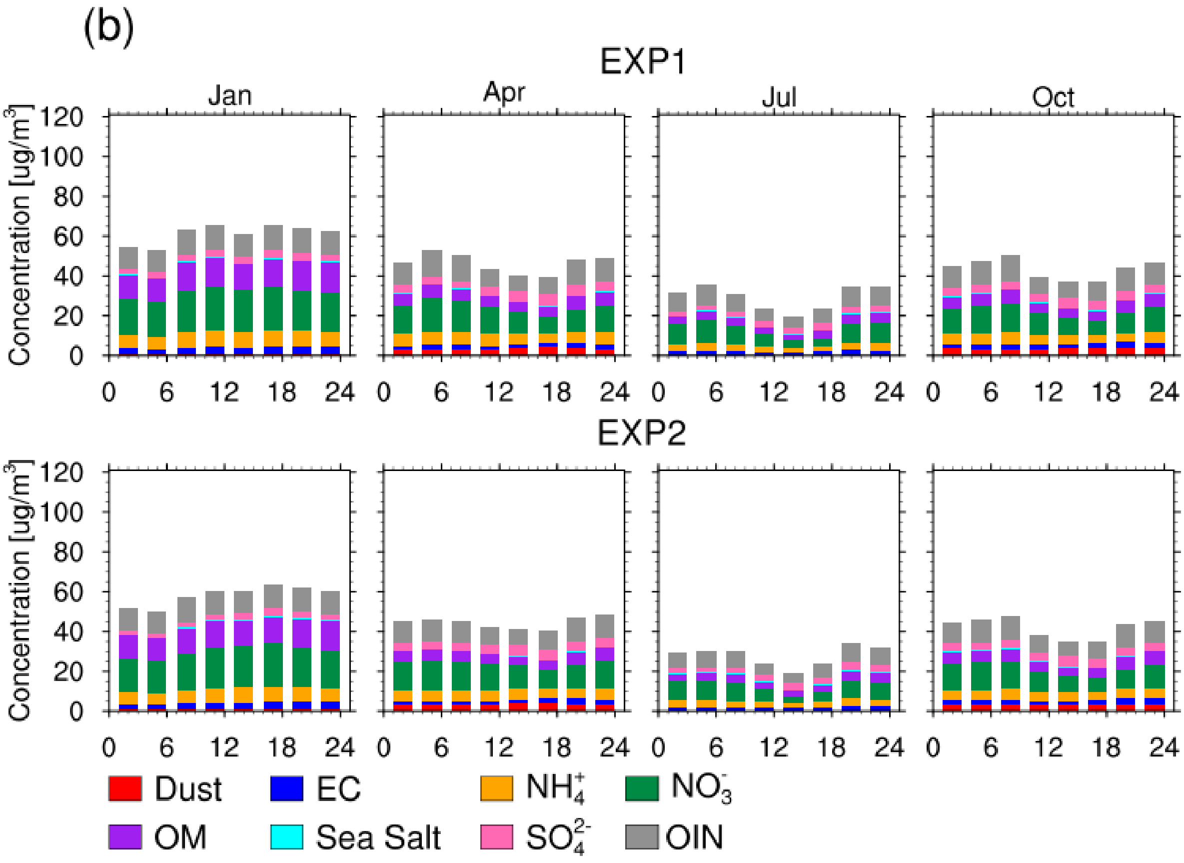

Figure S14b. Same as Fig. S14a but for Hangzhou.

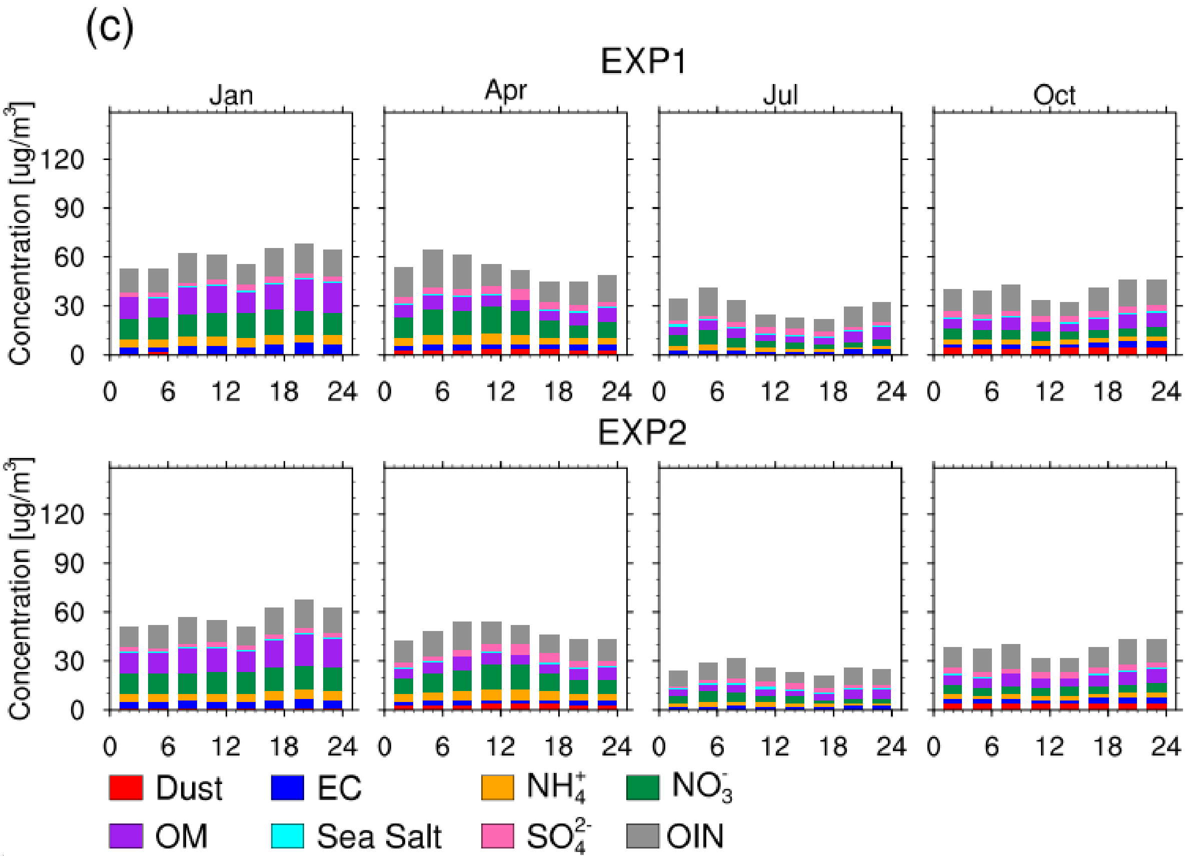

Figure S14c. Same as Fig. S14a but for Shanghai.

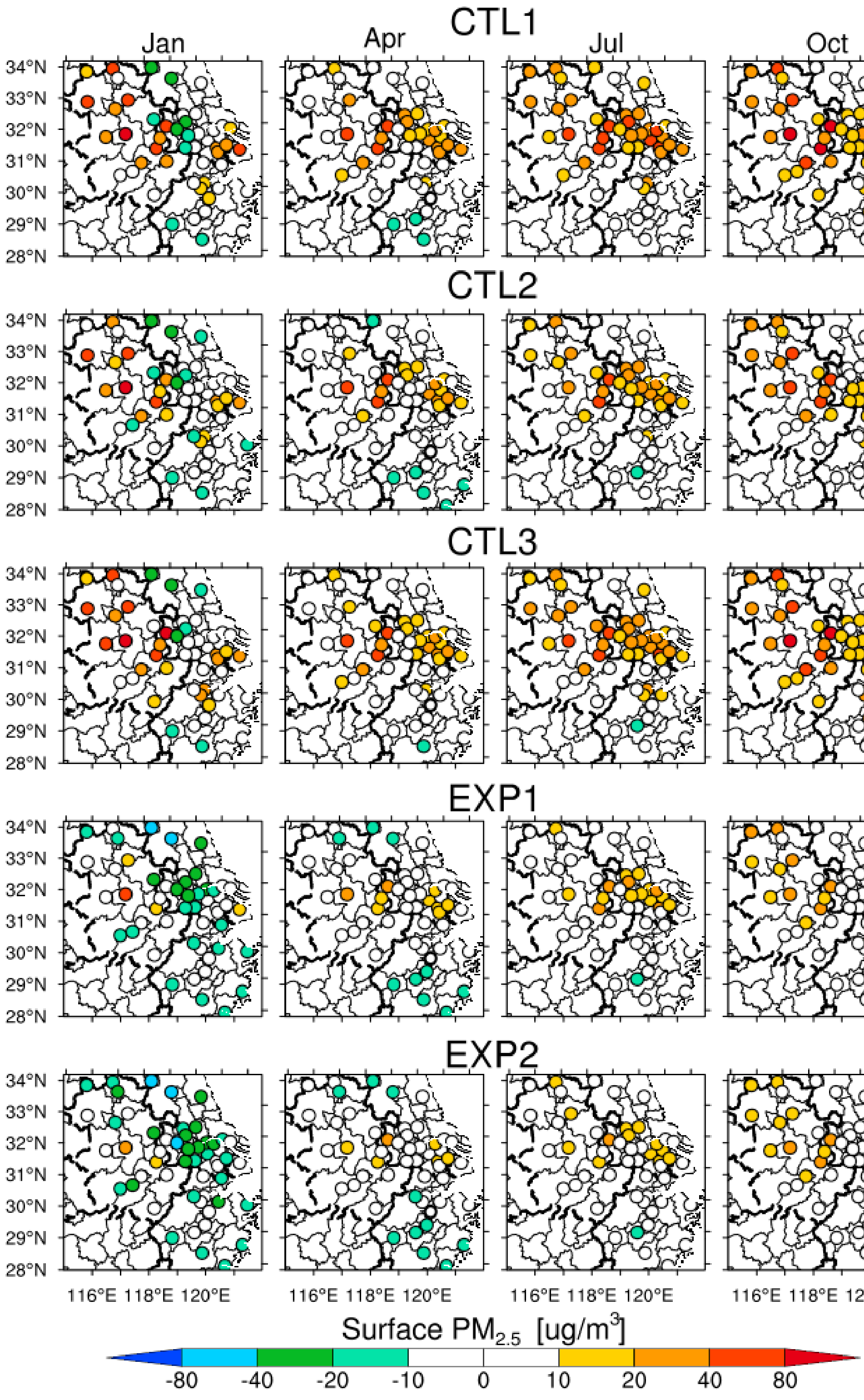

Figure S15. Spatial distribution of the difference in surface PM2.5 concentrations between experiments CTL1, CTL2, CTL3, EXP1, EXP2 and the observations at each station for January, April, July, and October of 2018.

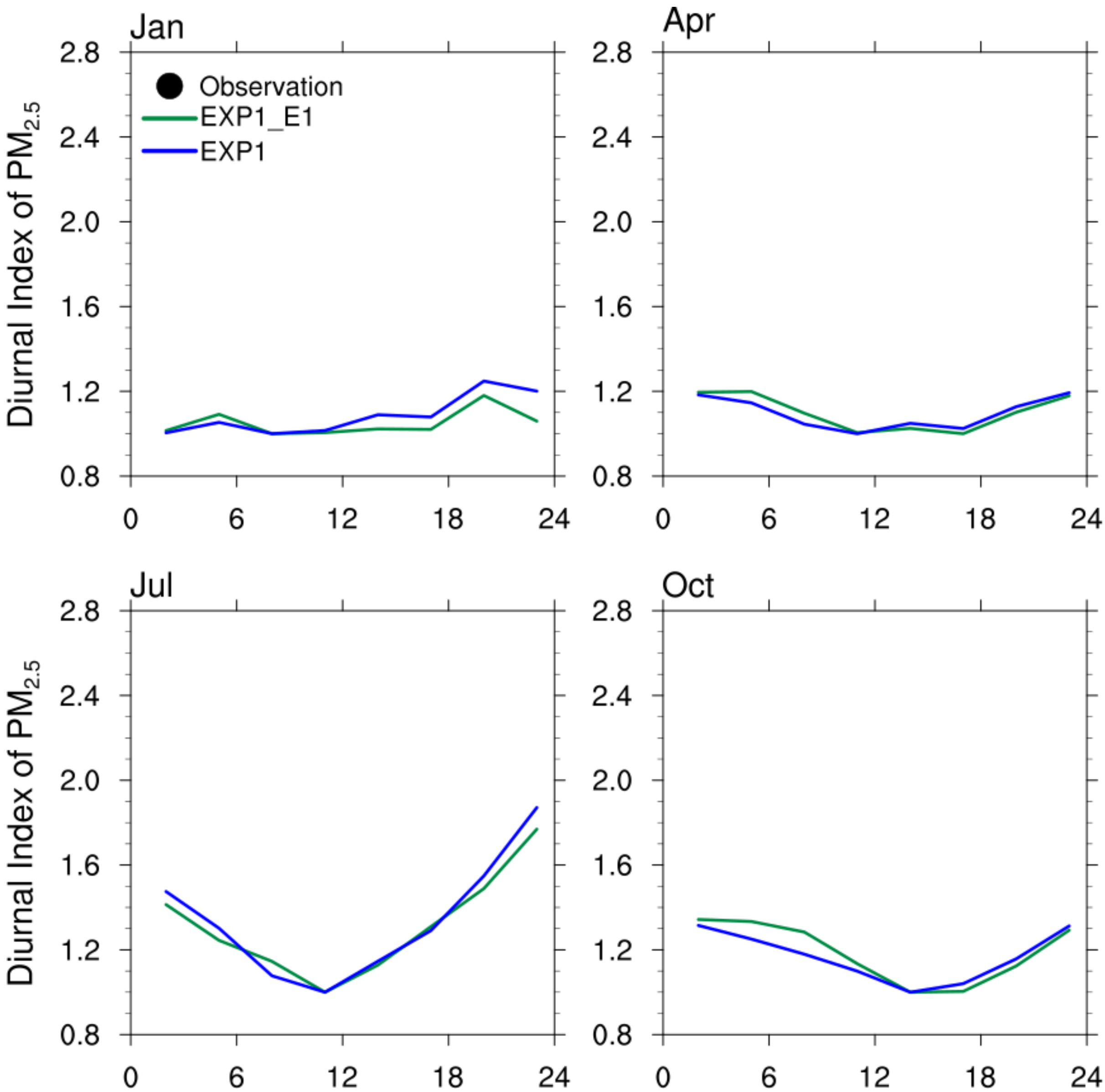

Figure S16. Diurnal index of surface $PM_{2.5}$ concentrations within 24-hour averaged over South Anhui for January, April, July, and October of 2018 from experiments EXP1_E1 and EXP1.

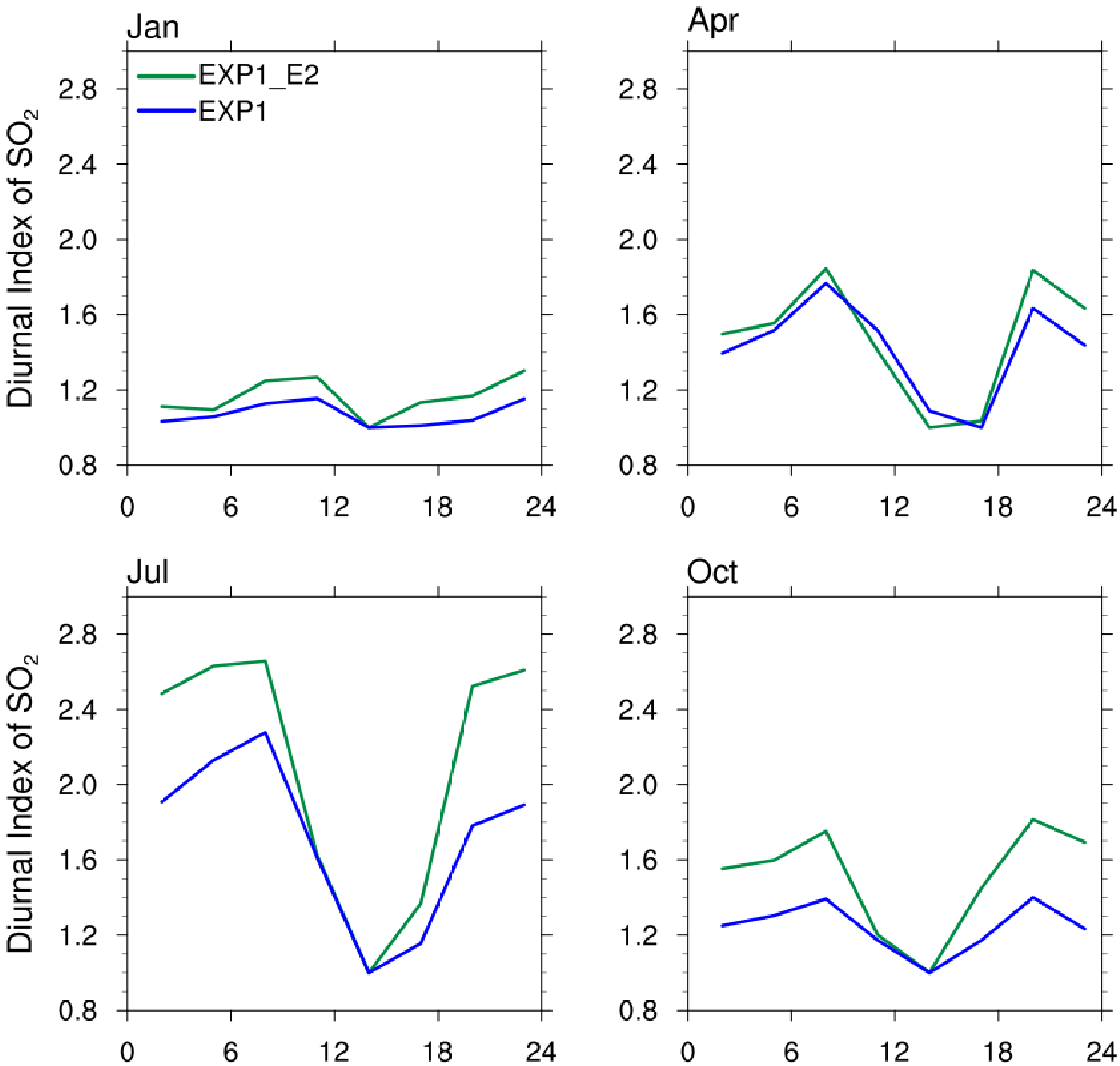

Figure S17. Diurnal index of surface SO_2 concentrations within 24-hour averaged over Nanjing, Jiangsunan power plant (118.76°E, 32.21°N) for January, April, July, and October of 2018 from experiments EXP1_E2, EXP1, and observations.

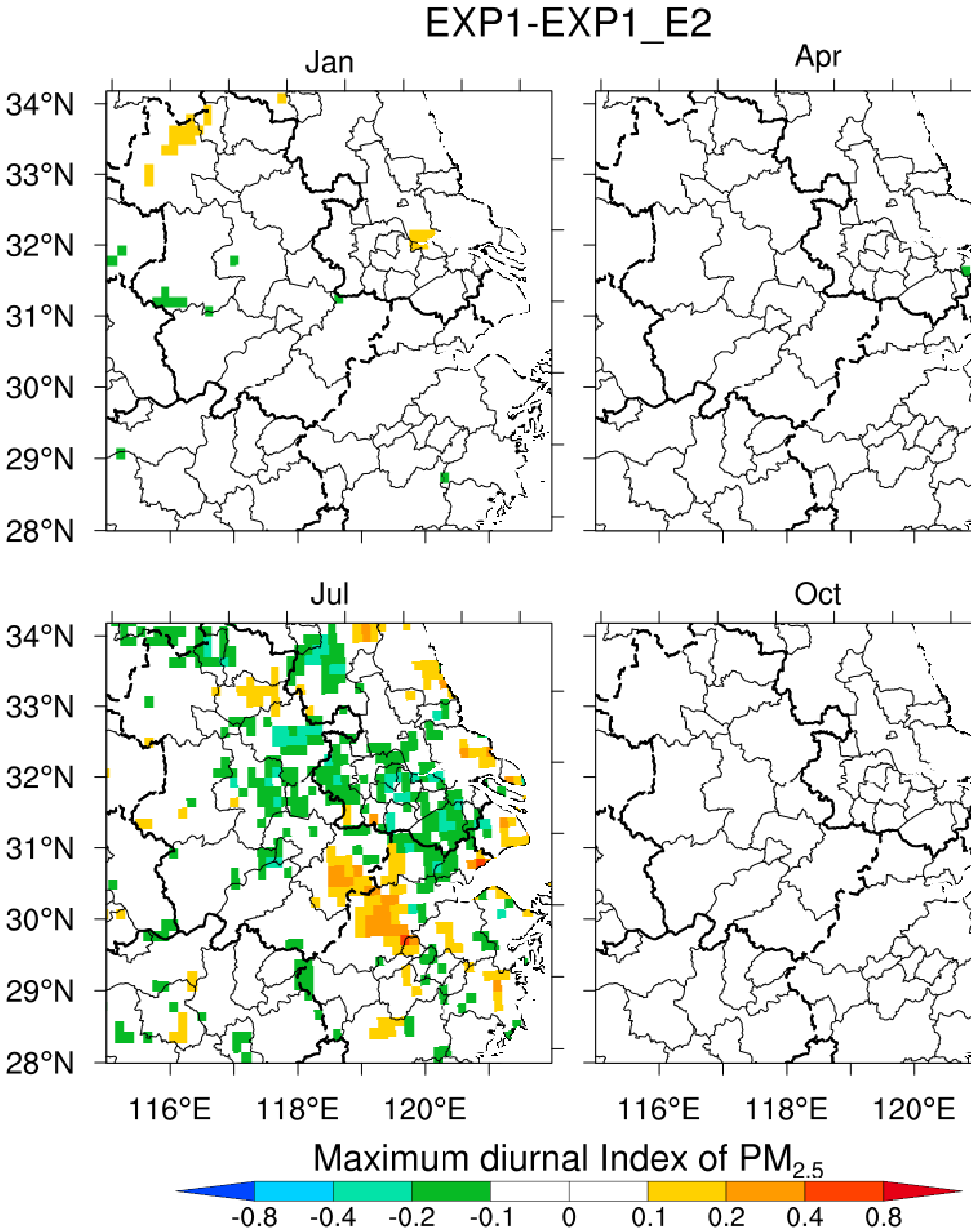

Figure S18. Spatial distribution of the difference in daily maximum diurnal index of surface $PM_{2.5}$ concentrations between experiments EXP1_E2 and EXP1 over East China in January, April, July, and October of 2018.

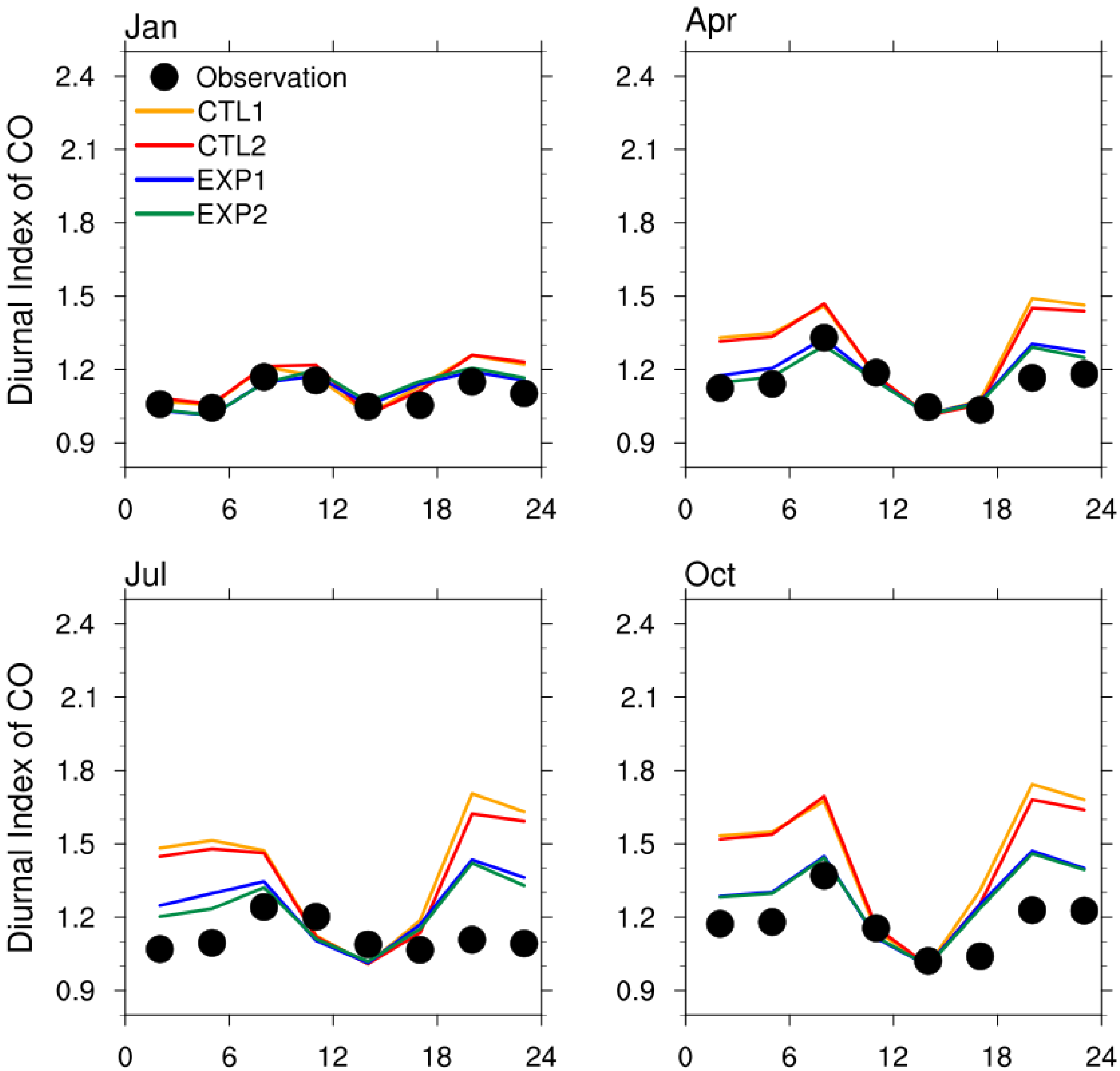

Figure S19. Diurnal index of surface CO concentrations within 24-hour averaged over the YRD region of East China (within black box of Fig. 1a) for January, April, July, and October of 2018 from experiments CTL1, CTL2, EXP1, EXP2, and observations.

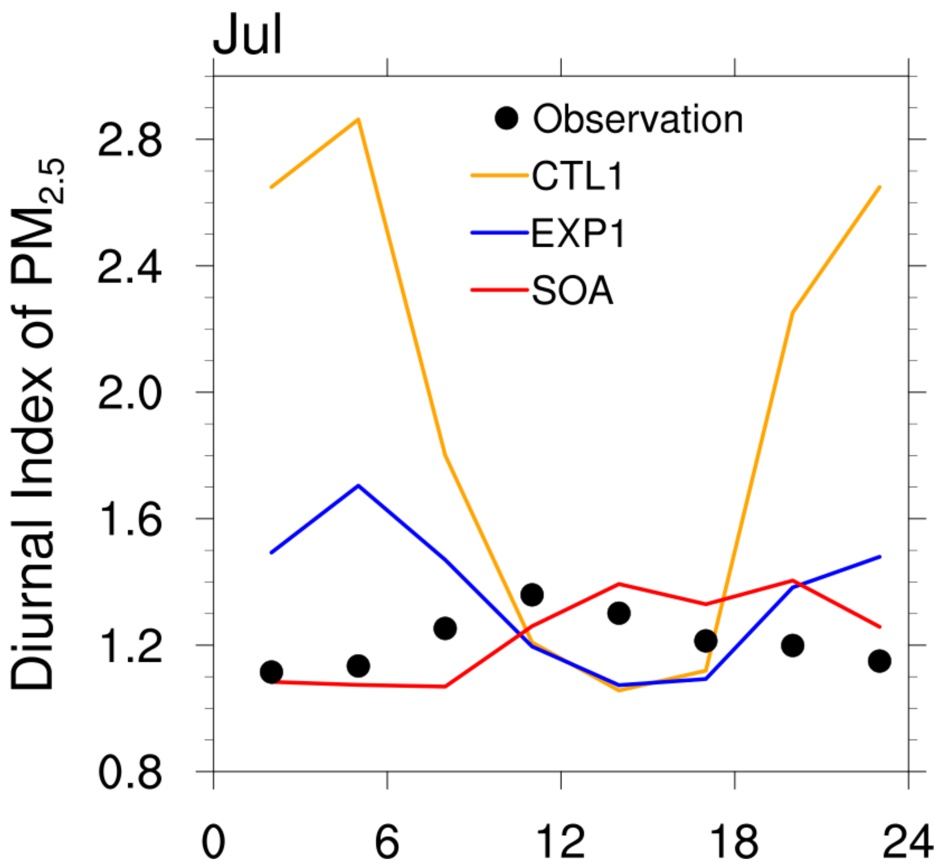

Figure S20. Diurnal index of surface $PM_{2.5}$ concentrations within 24-hour averaged over the YRD region of East China (within black box of Fig. 1a) for January, April, July, and October of 2018 from experiments CTL1, EXP1, SOA, and observations.